

# 3.0 Tesla

1. 1. 2. 1. 1. 1. 1. 1. 1. 2

: 3.0 Tesla  
 , Echo Planar Imaging(EPI) eddy current 가  
 가 slew rate 가  
 가 (Fast Spin Echo: FSE)  
 rf SAR 가  
 3.0  
 Tesla MRI  
 가  
 : 3 Tesla  
 . (higher-order) shimming  
 interleaves . gradient  
 , time repetition time, rf  
 (contrast)  
 : 3 Tesla  
 . (inhomogeneity) 가  
 shimming axial, sagittal,  
 coronal map spherical harmonics shimming  
 . in-vivo single shot 100×100  
 6-12 interleaves 256×256  
 : BOLD  
 가 rf field SAR  
 가 SAR 가  
 , EPI  
 . shimming , single shot  
 interleaving multi-shot 100×100 256×256  
 가

10:108-116(2006)

<sup>1</sup>VIA

<sup>2</sup>

: 2006 11 3 , : 2006 12 5  
 : 447-1  
 Tel. (02)940-5148 Fax. (02)909-3159 E-mail: cbahn@kw.ac.kr

k - space (1). dc [1] .  
 interleaving . K -  
 space (2), k - space ,  
 $k(t) = \varnothing(t)\exp(j\varnothing(t))$  [1]  
 $k(t) = k_x(t) + jk_y(t),$  .  $\varnothing(t)$   
 (11).  $\varnothing(t)$  grid  
 interpolation  
 EPI (3) eddy grid 가 , filtered  
 current , slew rate backprojection (1, 12).  $\varnothing$   
 rephasing 가 , (t) slew rate  
 (13). grid  
 coronary artery (4- griding  
 5). grid FFT  
 k - space (4, 6). Gridding  
 Fourier non uniform weight matrix  
 Transform (FFT) 가 weight [1]  
 interpolation grid matrix .  
 FFT filtered backprojection  
 (1, 6, 7).  
 (chemical shift) off - resonance  
 point spread 가 ring blur blur  
 가 . blur post  
 processing 가 (8, 9). Slew rate [2] .  
 f - MRI BOLD 가 , 가 ,  
 rf field slew rate  
 SAR  
 rf refocusing , , interleaves .  
 SAR  $T_2^*$   
 (10). k - space view matrix (N) (pixel ) field - of -  
 SAR N k - space N/(2M) , N x  
 single - shot M interleaves N/(2M) 가  
 interleaved , repetition time, time, rf angle sine cosine . Interleaving  
 [1] (= 2 / M)  
 interleaves (M) , N/(2M)  
 interleaves field - of -  
 view slew rate 가  
 , 가

matrix interleaves 가 , 1(b) rf -  
 gradient - rf 가  
 1 (a) gradient -

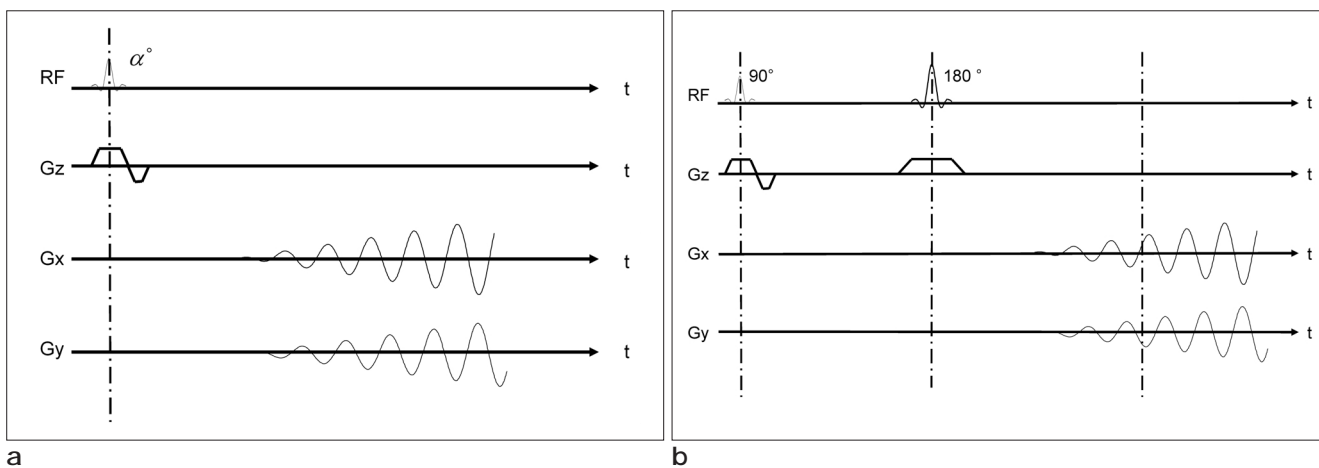


**Fig. 1.** Pulse sequences for spiral-scan imaging. (a) Gradient-echo based spiral-scan imaging sequence. (b) Spin-echo based spiral-scan imaging sequence.

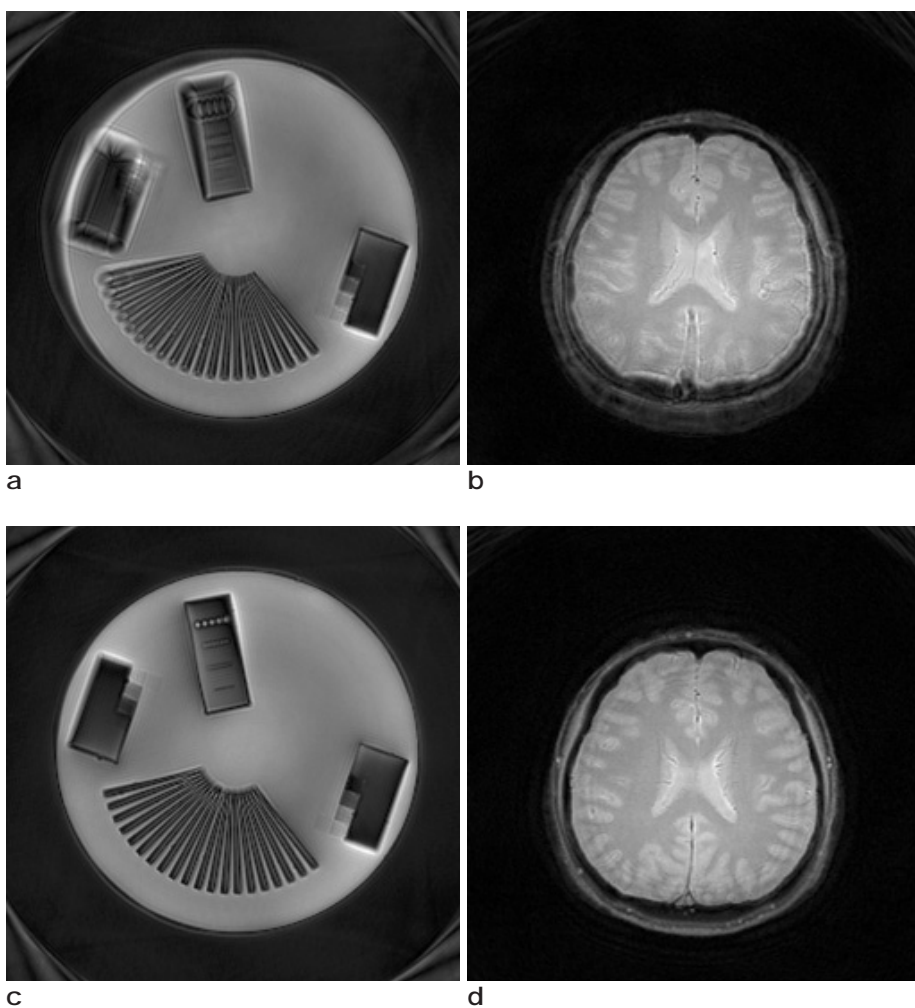


**Fig. 2.** Phantom and in-vivo head images obtained by the spiral-scan imaging at 3T whole body MRI system after the linear shimming only (a) and (b), and the linear and higher order shimming (c) and (d). Image blurs are observed in (a) and (b), while such blurs are mostly disappeared in (c) and (d).

3.0 Tesla

long  $T_2$

spherical harmonics

spherical harmonics

shim power supply

Higher order shimming

shim coil

(spherical

[ppm]

ppm

harmonics)

shimming

$T$

$2$   
가 eddy current

shimming

가

가  
( shimming)  
yz, zx

shimming  
shim coil

interleaves

x, y, z  
 $z^2, x^2 - y^2, xy,$

가  
autocorrelation  
(14).

가  
histogram  
map

map

map

axial, sagittal, coronal

shimming

shimming

refocusing

$T$

shimming

$2$

$2(a)$

(b)

$T =$

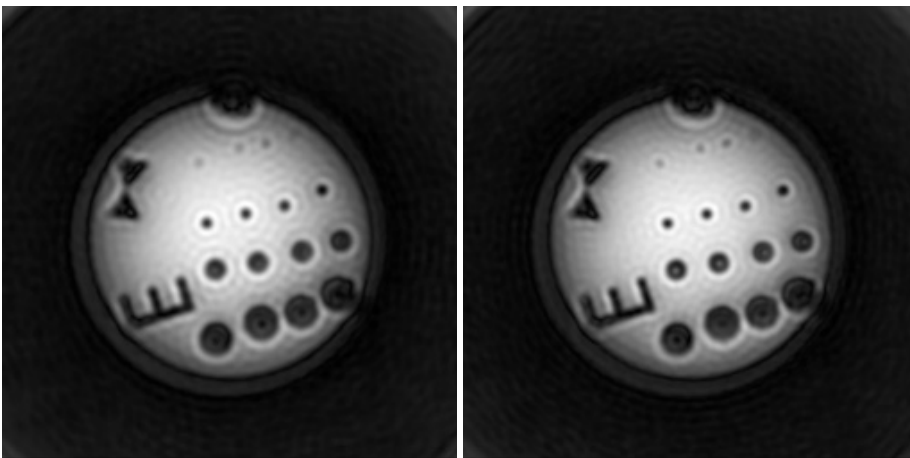
shimming  
2(c) (d)

shimming

shimming

2(a)

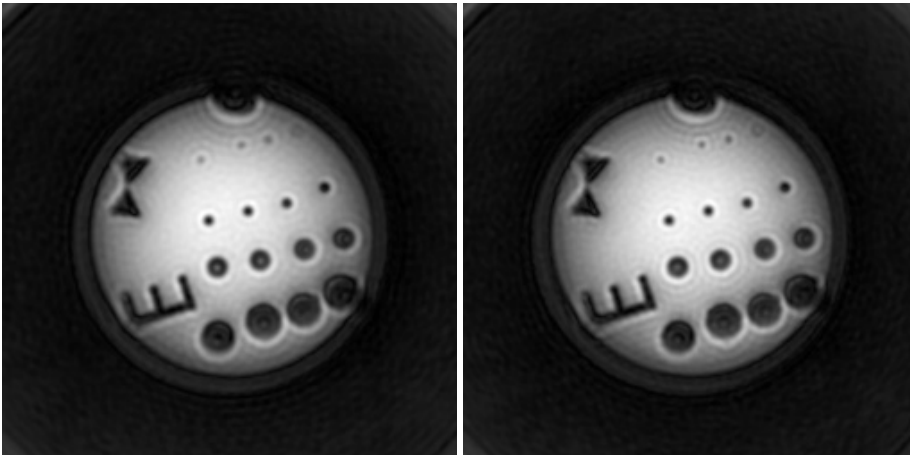
0



a

b

Fig. 3. Phantom images obtained by the single-shot spiral-scan technique with various experimental parameters. The gradient strength was 1.6 [Gauss/cm] and the slew rate was 7000 [Gauss/cm/s]. The image matrix size and acquisition duration are: (a)  $80 \times 80$ , 38.8 ms, (b)  $90 \times 90$ , 46.7 ms, (c)  $100 \times 100$ , 55.4 ms, (d)  $110 \times 110$ , 65.1 ms, respectively. Note the improved resolution with larger image matrix size, however, inhomogeneity effects are increased with longer acquisition durations.



c

d

repetition time 59.3 ms, matrix 80 × 80, 4 image blur EPI, N/2 ghost (15) 가, 5 interleaves 12, in - vivo volunteer, Repetition time 4s, 3 mm, matrix 256 × 256, rf 90 °, 5 interleave 가, 3 single - shot, 1.6 [Gauss/cm], gradient - 7 ms, proton density 가, 5(a) time, slew rate 7000 [Gauss/cm/s], matrix (a) 80 × 80, 38.8 ms (b) 90 × 90, 46.7ms, 5(b) gradient - time 80 ms, T<sub>2</sub>\* 가, 3 가 (slew rate matrix 5(c) time pixel 가) 120 ms, 5(c) T<sub>2</sub>, matrix 가, 가, gradient -, single - shot, image blur 가, 4 (5(b)) long time 가, 3 mm, rf 90 °, time f - MRI, BOLD susceptibility gradient -, 40 ms, oblique 12 °, single shot,

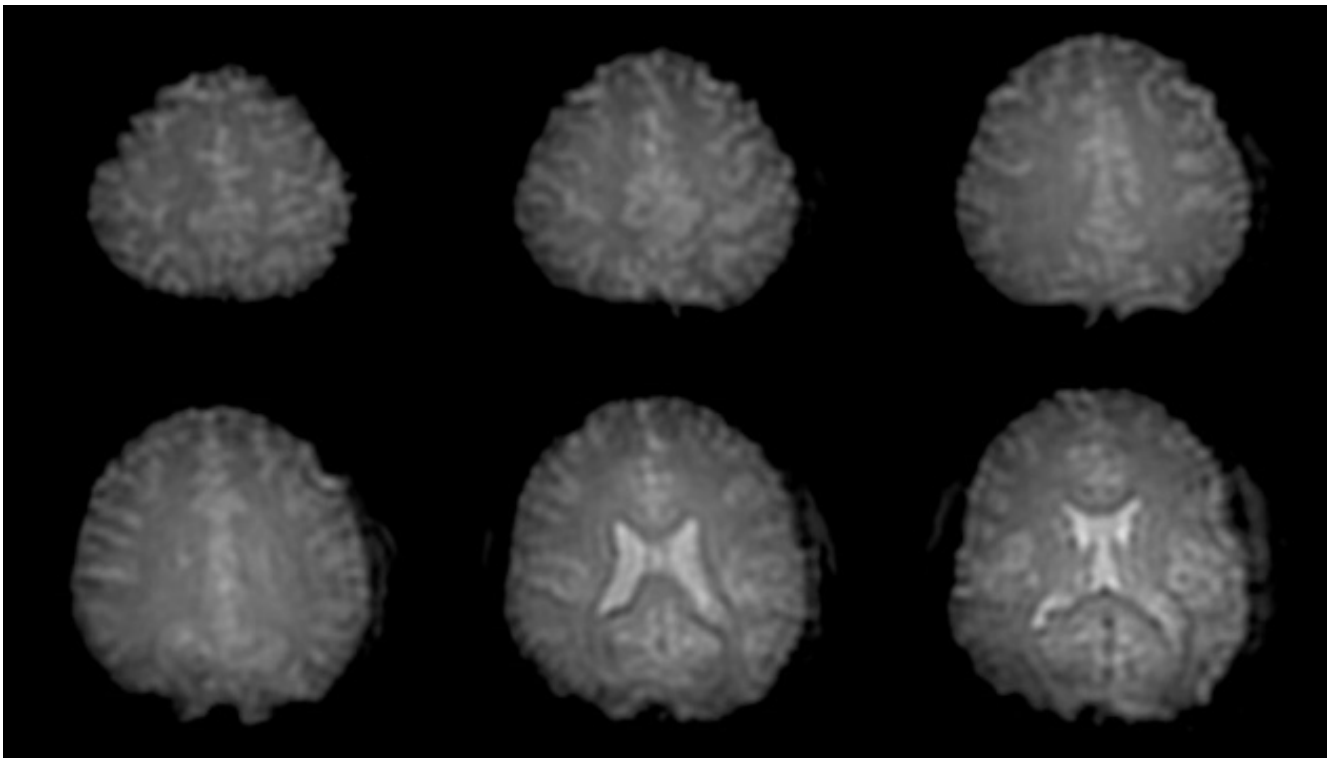


**Fig. 4.** In-vivo multi-slice head images obtained by the single-shot spiral-scan method. Rf flip angle was 90 °, echo time was 40 ms, and oblique selection angle was 12 °. The repetition time was infinite for a single-shot scan. Data acquisition duration was 59.3 ms, the slice thickness was 3 mm, and the image matrix size was 80 × 80.

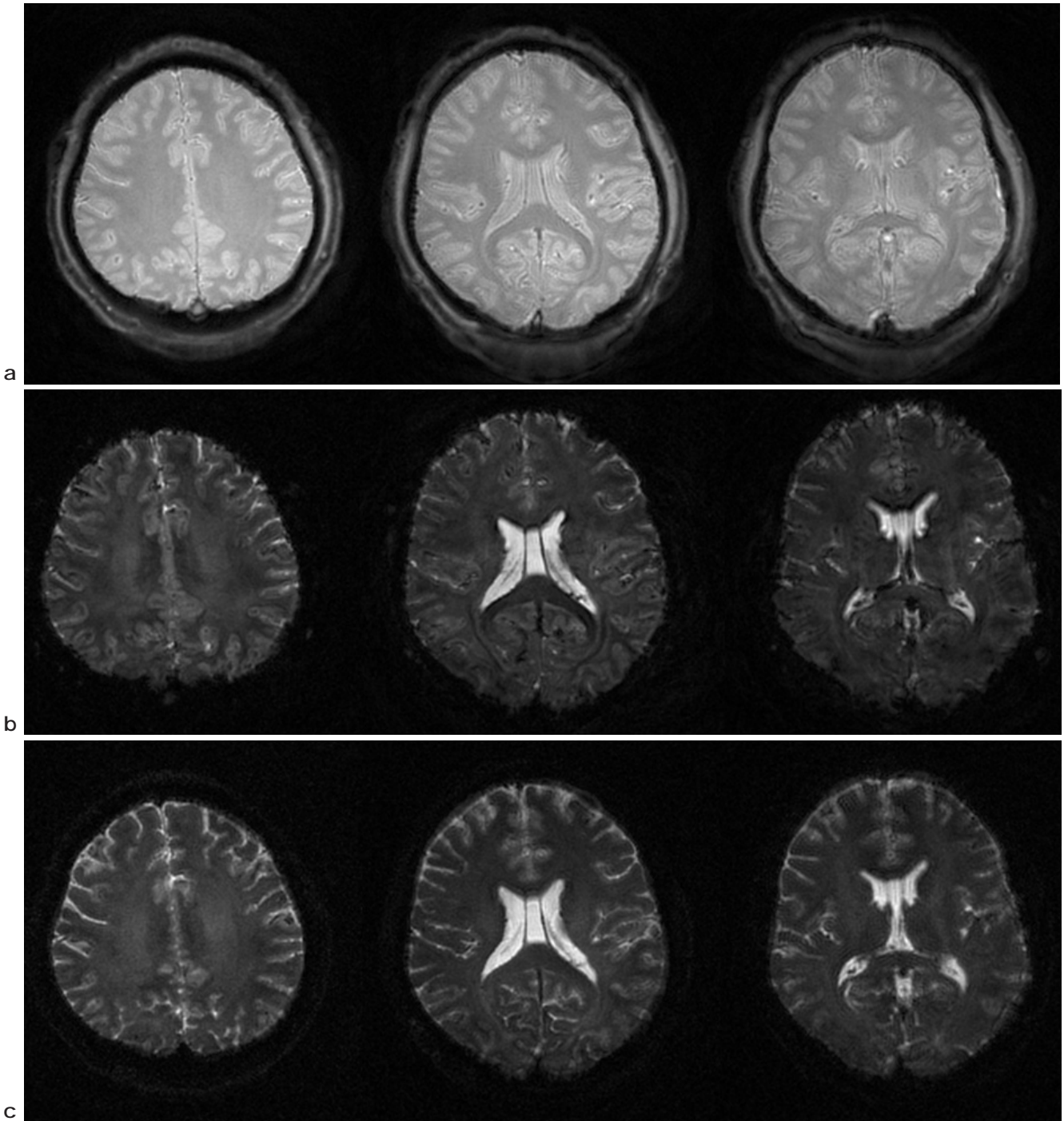


**Fig. 5.** High-resolution in-vivo head images obtained by the spiral-scan imaging with 12 interleaves. Image matrix size was  $256 \times 256$ , slice thickness was 3 mm, repetition time was 4s, and the rf flip angle was  $90^\circ$ . (a) Images obtained by the gradient-echo based spiral-scan sequence with the echo time of 7 ms, (b) images obtained by the gradient-echo based spiral-scan sequence with the echo time of 80 ms, and (c) images obtained by the spin-echo based spiral-scan sequence with the echo time of 120 ms. Note the heavy T2 contrasts in (b) and (c).

가 . gradient - , interleaves  
 6 repetition time 1s, time 7 ms , 12 , matrix  $256 \times 256$  . 6(a) rf  
 rf .  $90^\circ$  . repetition

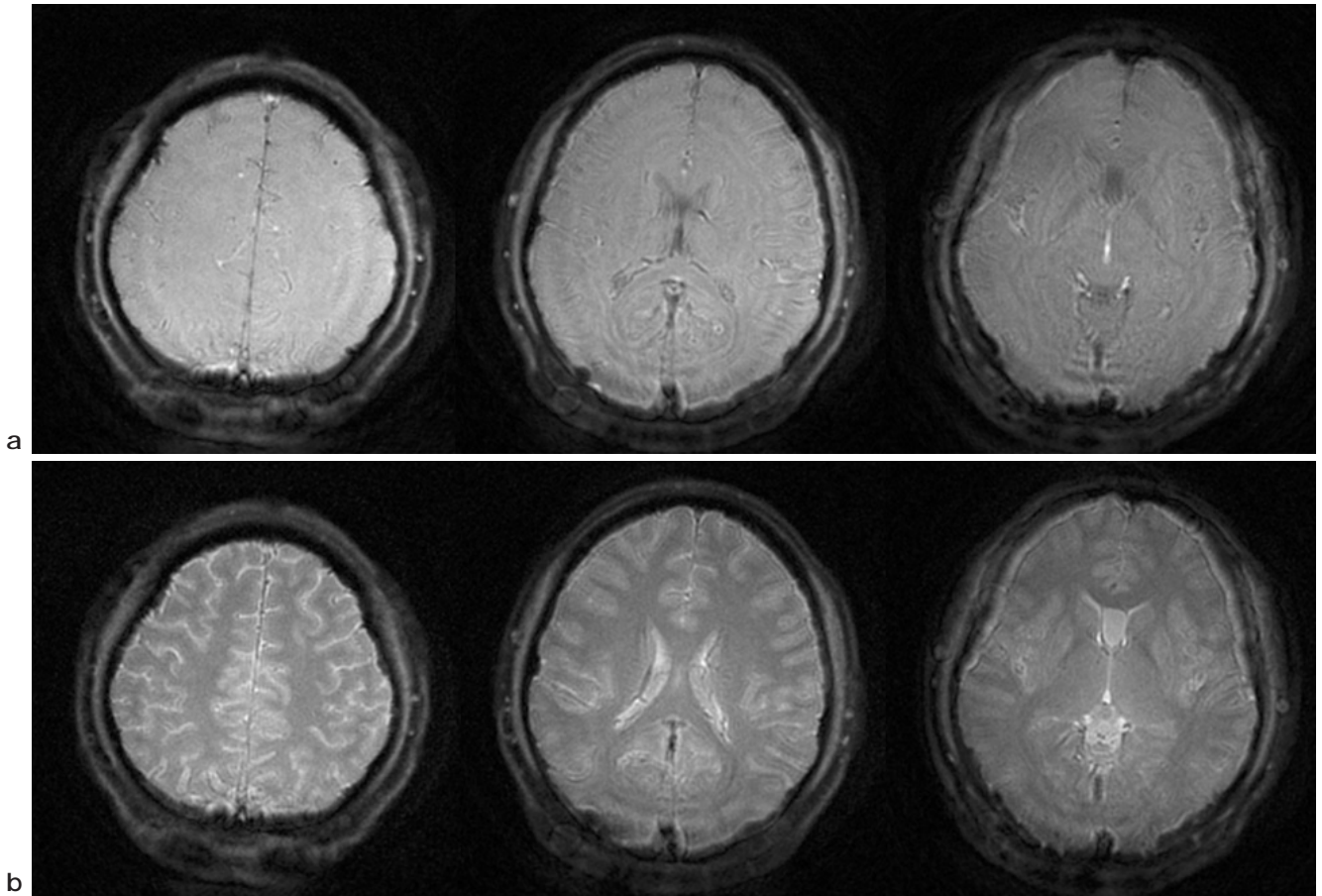


Fig. 6. High-resolution in-vivo multi-slice head images obtained by the interleaved spiral-scan method with 12 interleaves. Image matrix size was  $256 \times 256$ , repetition time was 1s, and the rf flip angles were  $90^\circ$  (a) and  $30^\circ$  (b), respectively. Note the improved image contrast with the rf flip angle of  $30^\circ$  in (b).

time	time	$T_1$	$T_2$	가	rf field	SAR	가가	
.	6(b) rf	가	5(a) repetition time	가	eddy current	SAR	가	EPI
4s	,	30°	.	rf	가	가	slew rate	가
가	,	repetition time	7	3T	Tesla	가	.	3
multi - slice in - vivo	.	12	coronal	map	axial, sagittal,	가	spherical harmonics	
,	256	180° rf	가	shimming	in - vivo	가	interleaving	
rf	12	30° rf	SAR	single shot	interleaving	100 x 100	256 x	
.	.	.	.	multi - shot	100 x 100	Rf	.	
				256	repetition time	가		
				60 ms	10	single - shot	(~100 x	SAR
, BOLD				100)	multi - slice	(256 x 256)		
가	.	.	.	.	.	.	.	.

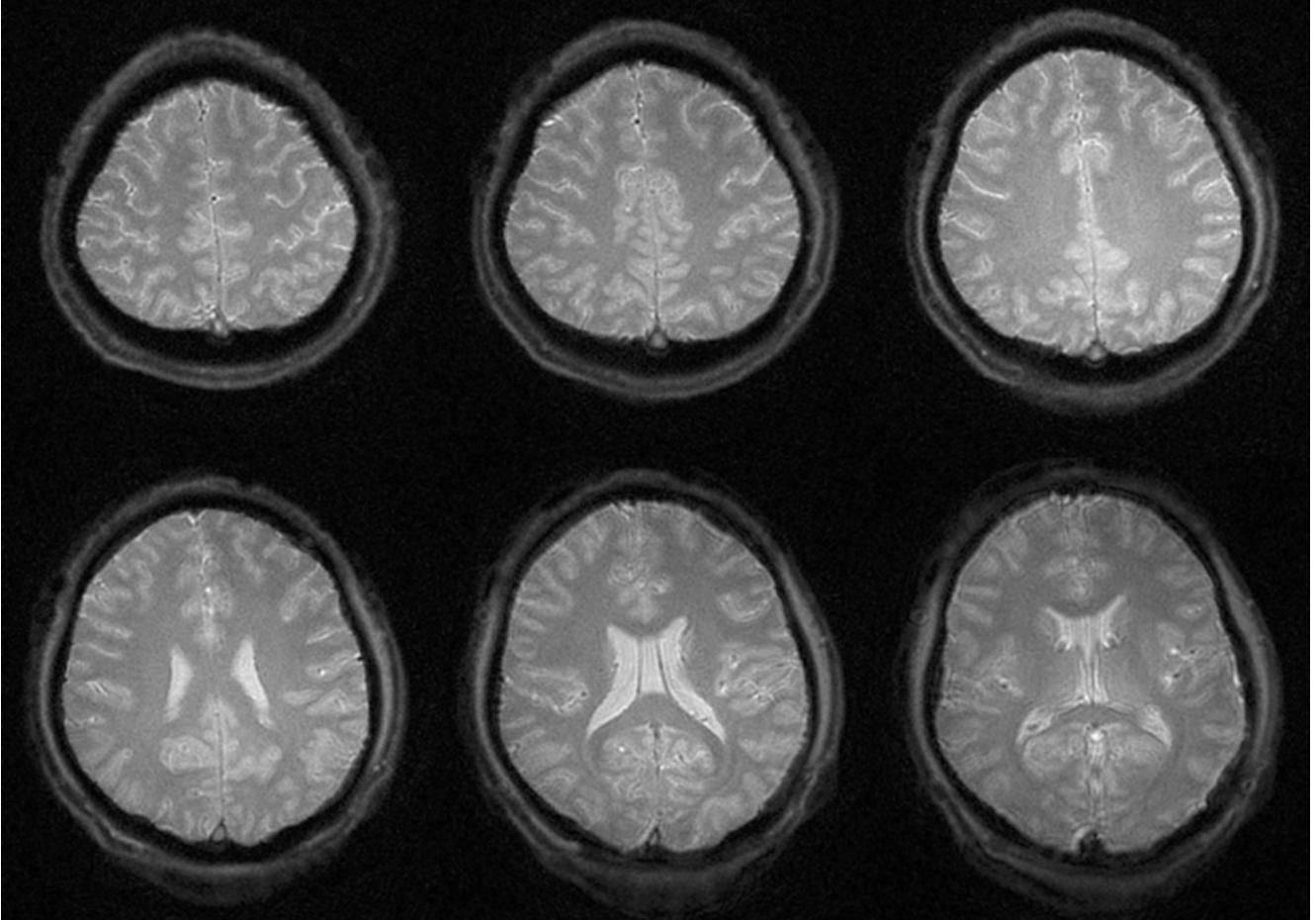


Fig. 7. High-resolution in-vivo multi-slice head images obtained by the interleaved spiral-scan method with 12 interleaves. Image matrix size was  $256 \times 256$ , repetition time was 1s, and the rf flip angle was  $30^\circ$ . Total measurement time was 12s.

1. Ahn CB, Kim JH, Cho ZH. High-speed Spiral-Scan Echo Planar NMR Imaging-I. *IEEE Trans Med Imag* 1986;5:1-6
2. Ljunggren S. A simple graphical representation of Fourier-based imaging methods. *J Magn Reson* 1983;54:338-343
3. Mansfield P. Multi-planar image formation using NMR spin echoes. *J Phys C* 1977;10:155-158
4. Meyer CH, Hu BS, Nishimura DG, Macovski A. Fast Spiral coronary artery imaging. *Magn Reson Med* 1992;28:202-213
5. Nishimura DG, Irarrazabal P, Meyer CH. A velocity k-space analysis of flow effects in Echo Planar and Spiral Imaging. *Magn Reson Med* 1995;33:549-556
6. Jackson J, Meyer CH, Nishimura DG, Macovski A. Selection of a convolution function for Fourier inversion using gridding. *IEEE Trans Med Imag* 1991;10: 473-478
7. Ahn CB, Kim HJ, Oh CH, Kim CY. Reconstruction aspects of Spiral Scan magnetic resonance imaging. *Proc. SPIE, Med Imag* 1998;3336:141-152
8. Noll DC, Pauly JM, Meyer CH, Nishimura DG, Macovski A. Deblurring for non-2D Fourier transform magnetic resonance imaging. *Magn Reson Med* 1992;25:319-333
9. Moriguchi H, Dale BM, Lewin JS, Duerk JL. Block regional off-resonance correction (BRORC): A fast and effective deblurring method for spiral imaging. *Magn Reson Med* 2003;50:643-648
10. Hennig J, Scheffler K. Hyperechoes in RARE/(TSE, FSE)-sequences. *Proc. Intl. Soc. Mag Reson Med* 2001;9:1769
11. Bernstein MA, King KF, Zhou XJ. *Handbook of MRI Pulse Sequences*. New York: Elsevier, 2004
12. . . . . - Echo Planar Spiral Scan . . . . . 1999;3:6-11
13. Glover GH. Simple analytic spiral k-space algorithm. *Magn Reson Med* 1999;42:412-415
14. Ahn CB, Cho ZH. A new phase correction method in NMR imaging based on autocorrelation and histogram analysis. *IEEE Trans Med Imag* 1987;6:32-36
15. Schmitt F, Stehling MK, Turner R. *Echo-Planar Imaging: Theory, Technique and Application*. Berlin: Springer, 1998



## High-resolution Spiral-scan Imaging at 3 Tesla MRI

C.B. Ahn<sup>1</sup>, P.K. Kim<sup>1</sup>, J.W. Lim<sup>2</sup>, S.W. Kang<sup>1</sup>, S.H. Cho<sup>1</sup>, S.Y. Jeon<sup>1</sup>,  
H.J. Lim<sup>1</sup>, H.C. Park<sup>1</sup>, S.J. Oh<sup>1</sup>, H.K. Lee<sup>2</sup>

<sup>1</sup>VIA-Multimedia Center, Kwangwoon University

<sup>2</sup>ISOL Technology Co.

**Purpose :** High-resolution spiral-scan imaging is performed at 3 Tesla MRI system. Since the gradient waveforms for the spiral-scan imaging have lower slopes than those for the Echo Planar Imaging (EPI), they can be implemented with the gradient systems having lower slew rates. The spiral-scan imaging also involves less eddy currents due to the smooth gradient waveforms. The spiral-scan imaging method does not suffer from high specific absorption rate (SAR), which is one of the main obstacles in high field imaging for rf echo-based fast imaging methods such as fast spin echo techniques. Thus, the spiral-scan imaging has a great potential for the high-speed imaging in high magnetic fields. In this paper, we presented various high-resolution images obtained by the spiral-scan methods at 3T MRI system for various applications.

**Materials and Methods :** High-resolution spiral-scan imaging technique is implemented at 3T whole body MRI system. An efficient and fast higher-order shimming technique is developed to reduce the inhomogeneity, and the single-shot and interleaved spiral-scan imaging methods are developed. Spin-echo and gradient-echo based spiral-scan imaging methods are implemented, and image contrast and signal-to-noise ratio are controlled by the echo time, repetition time, and the rf flip angles.

**Results :** Spiral-scan images having various resolutions are obtained at 3T MRI system. Since the absolute magnitude of the inhomogeneity is increasing in higher magnetic fields, higher order shimming to reduce the inhomogeneity becomes more important. A fast shimming technique in which axial, sagittal, and coronal sectional inhomogeneity maps are obtained in one scan is developed, and the shimming method based on the analysis of spherical harmonics of the inhomogeneity map is applied. For phantom and in-vivo head imaging, image matrix size of about  $100 \times 100$  is obtained by a single-shot spiral-scan imaging, and a matrix size of  $256 \times 256$  is obtained by the interleaved spiral-scan imaging with the number of interleaves of from 6 to 12.

**Conclusion :** High field imaging becomes increasingly important due to the improved signal-to-noise ratio, larger spectral separation, and the higher BOLD-based contrast. The increasing SAR is, however, a limiting factor in high field imaging. Since the spiral-scan imaging has a very low SAR, and lower hardware requirements for the implementation of the technique compared to EPI, it is suitable for a rapid imaging in high fields. In this paper, the spiral-scan imaging with various resolutions from  $100 \times 100$  to  $256 \times 256$  by controlling the number of interleaves are developed for the high-speed imaging in high magnetic fields.

**Index words :** Spiral-scan imaging, fast magnetic resonance imaging,  
specific absorption rate (SAR), higher order shimming, slew rate

Address reprint requests to : Chang Beom Ahn, Ph.D., VIA-Multimedia Center, Kwangwoon University  
447-1 Wolgye-dong, Nowon-gu, Seoul 139-701, Korea  
Tel. 82-2-940-5148 Fax. 82-2-909-3159 E-mail: cbahn@kw.ac.kr